Conf-830406--45

Paper to be presented at Fifth Topical Meeting on the Technology of Fusion Energy, Knoxville, Tennessee, April 26-28, 1983; and for publication in Nuclear Technology/Fusion.

CONF-830406--45

DE83 011695

# MECHANICAL DESIGN AND THERMAL HYDRAULIC CONSIDERATIONS FOR SELF-COOLED LITHIUM-LEAD BLANKET*

B. Misra and D. L. Smith
Fusion Power Program
Argonne National Laboratory
Argonne, Illinois 60439

R. C. Burk and G. D. Morgan
Fusion Energy
McDonnell Douglas Astronautics Company
P. O. Box 516
St. Louis, Missouri 63166



Submitted March 1983



*Work supported by the U. S. Department of Energy.

EBB

# MECHANICAL DESIGN AND THERMAL HYDPAULIC CONSIDERATIONS FOR A SELF-COOLED LITHIUM-LEAD BLANKET

B. MISRA and D. L. SMITH, Fusion Power Program
Argonne National Laboratory
Argonne, Illinois 60439
(312)/972-4513/972-5180

R. C. BURK and G. D. MORGAN, Fusion Energy
McDonnell Douglas Astronautics Company
P. O. Box 516, St. Louis, Missouri 63166
(314)/234-1213/576-8273

ABSTRACT

Liquid lithium-lead eutectic alloy (17 at-% Li-83 at-% Pb, referred to herein as Li-Pb) is currently being considered as a candidate breeding material for fusion reactors. Some important considerations in the design of a Li-Pb blanket are compatibility with the structure, tritium containment and recovery, and safety. Additional design complexities arise because of the high density of Li-Pb, the relatively high melting temperature (235°C), and the high tritium overpressure associated with this alloy. In this study, the Li-Pb eutectic was considered both as the breeder and as the coolant. Thermal hydraulic and stress analyses were conducted to assess the technical feasibility of using Li-Pb as the breeder and coolant based on DEMO reactor conditions. The results of the thermo-mechanical analyses showed that the elongated cylindrical blanket modules made from either HT-9 or vanadium alloy offer a viable first wall/blanket design concept.

INTRODUCTION

Deuterium-tritium fueled fusion power reactors must breed tritium in order to be economically viable. Hence, tritium breeding and extraction must be an integral part of reactor design. Solid lithium compounds, liquid lithium-lead alloys, and liquid lithium have been considered as the breeding materials.[1-5] One objective of the DEMO study was to evaluate the potential of the Li-Pb in a tritium breeding blanket. Tritium containment and extraction, heat transport and power conversion cycle, and magnetohydrodynamic effects with heat transfer and fluid flow are important considerations in the blanket design. The use of Li-Pb as a breeder material requires consideration of breeder structure compatibility. The use of another material as coolant introduces several other compatibility issues, viz., coolant/breeder and coolant/structure compatibility. Although the lack of a broad data base for Li-Pb precludes full consideration of the above issues, a number of these issues were addressed to a significant extent in the DEMO study.[4] The purpose of this paper is to assess the viability of self-cooled Li-Pb blankets of radial flow design over a limited range of operating conditions. The analyses considered both the thermal hydraulic and structural design aspects as described in the following sections. For this study both ferritic steels (e.g., HT-9) and vanadium alloys (e.g., V-15- Cr-5Ti) were considered as structural materials for Li-Pb blankets, since these materials offer the greatest potential.

DESIGN CONSIDERATIONS

Self-cooling by the Li-Pb alloy presents a number of problems. The high density of the coolant (~10 g/cc) leads to very large gravity loads and static pressure head. In addition, induced MHD forces are large due to Li-Pb being an electrically conducting liquid. The corrosion product mass transfer problems in a flowing system limit the operating temperature. The low solubility of tritium in Li-Pb has a positive effect on tritium extraction. However, it results in high tritium overpressure, thus making tritium containment more difficult. The high melting point of Li-Pb (235°C) may lead to requirements for auxiliary heaters, an added design complexity. The reactivity of Li-Pb alloy with water leads to safety concerns for the intermediate loop or double wall tube heat exchangers. Pumping of heavy liquid metals such as 17Li-83Pb in and around magnetic fields is an unproven technology. On balance, however, self-cooling by Li-Pb offers very significant design simplifications. Hence, a series of parametric thermal hydraulic and stress studies were carried out for a liquid Li-Pb alloy self-cooled blanket design. Corrosion compatbility limits are projected to place a maximum operating temperature of 450-500°C for HT-9 and 550-600°C for the V-alloys.

The blanket design objectives were to produce a blanket module with: (1) high coolant temperatures to maximize thermodynamic efficiency; (2) low coolant flow rates to minimize pumping power losses; (3) high breeder to structure material ratio to yield adequate tritium breeding; (4) compact size to reduce blanket material and tritium inventory; (5) low structure material temperature to increase blanket life and to reduce tritium permeation; and (6) overall plant safety. Since a large number of constraints have been placed on the Li-Pb blanket design, as discussed in foregoing sections, the full potential of self-cooled Li-Pb blankets may not be realized.

## MODEL FOR THERMAL HYDRAULIC/STRUCTURAL ANALYSIS

Figure 1 presents a schematic drawing of the reference self-cooled blanket module analyzed herein. The elongated radial-flow cell shown is similar to the STARFIRE backup lithium blanket concept[2] and to the lithium-cooled module concept in Ref. 5. The semi-cylindrical heads form the first wall, which is cooled from the back side by flowing Li-Pb. The Li-Pb enters through a standpipe, flows from a manifold through the gap between a baffle and the first wall, then reenters the chamber from which it is withdrawn through holes in the cell's rear wall. This concept minimizes voids in the regions which are available for breeding and also minimizes associated neutron streaming problems. The module walls are pressurized internally to ~1-2 MPa, because of (1) the Li-Pb static head resulting from interconnection of the blanket modules in the sector; (2) the pressure head needed to overcome the blanket MHD forces and system frictional losses; and (3) to pump the Li-Pb through the primary coolant systems. This pressure level requires that the internal frames be spaced relatively close together to break up the large-area flat walls into smaller panels.

The model for the thermal-hydraulic calculations is shown in Fig. 2. In this model it is assumed that the first wall has a beryllium coating for plasma impurity control. The calculations are based on the following data and operating conditions for the reference module:

| | |
|---|---|
| Surface heat flux, MW/m$^2$ | 0.5 |
| Nuclear heating rate, W/cc: | |
| Structural material (HT-9 or V-alloy) | 11.5 |
| Coolant (17Li-83Pb) | 22.2 |
| Be coating (70% dense) | 11.3 |
| Coolant temperature, °C: | |
| Inlet/outlet | 300/450 |
| Diameter of cylindrical heads, cm | 30 |
| Thickness of materials and coolant channel, mm: | |
| Be coating, first wall, coolant channel, baffle plate | 3 |

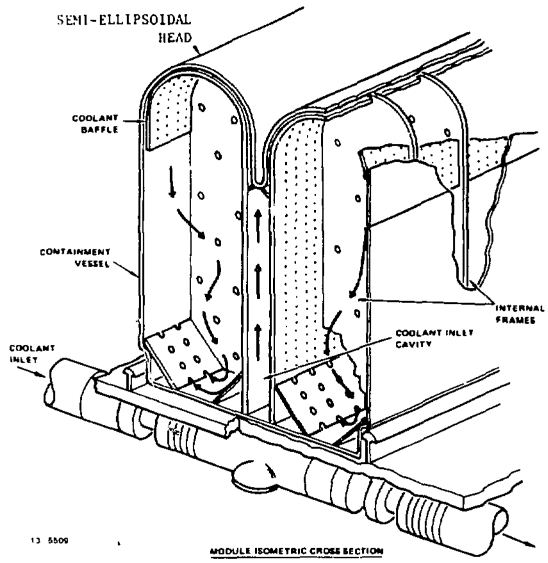


Fig. 1. Selected blanket design configuration for Li-Pb breeder/coolant approach.

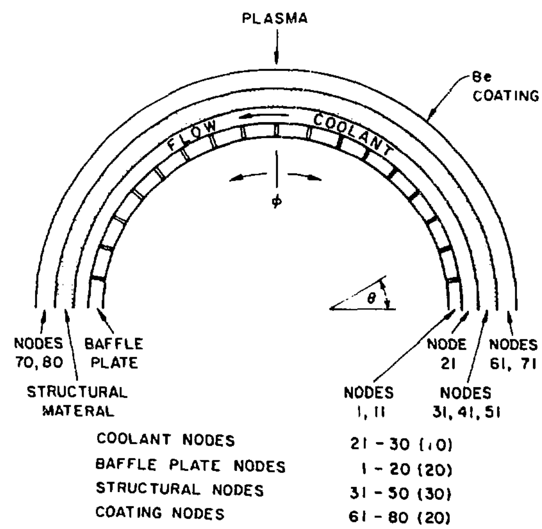


Fig. 2. Geometrical model.

The surface heat flux on the first wall is assumed to have a cos $\phi$ distribution ($\phi$ = angle *away from the midpoint of each semi-cylinder.* Assuming uniform flux distribution in the lengthwise direction of the blanket modules, the thermal analysis was carried out based on two-dimensional heat conduction. The module was divided into ten regions in the circumferential direction, with two layers in the beryllium coating, three in the structural material, one in the coolant, and two in the baffle plate. The baffle plate between the first wall and the blanket region is assumed to be perforated to prevent stagnant thermal regions behind the baffle.

RESULTS OF THERMAL/HYDRAULIC ANALYSIS

The steady-state temperature distribution for three thicknesses of HT-9 structure are given in Table I. Typical temperature plots for a selected set of nodes from the 80-node geometrical model for the 3-mm thickness reference case are shown in Figs. 3 and 4. The results show that ~33% of the total temperature rise of the coolant (20% due to surface heat flux and 13% due to bulk heating) occurs across the first wall. The maximum surface temperature of the structural material (HT-9) reaches ~415°C (obtained by extrapolation from nodes 47 and 57). The maximum surface temperature of the beryllium coating approaches 485°C. The maximum temperature of the structural material at the liquid metal interface occurs at the coolant exit where it approaches the coolant temperature.

The gravity load on a particular first wall/blanket module will depend on its location in the poloidal plane. Hence, the required material thickness will depend to some extent on the location of the modules. A set of calculations was carried out by varying the thickness of the first wall to estimate how the material thickness affects the temperature distribution. When this thickness is increased from 3 to 4.5 mm, and then to 6 mm, the maximum structural material temperature is increased by 33°C and 75°C, respectively. An examination of the circumferential temperature distribution shown in Fig. 4

TABLE I

Steady-State Temperature Distribution in Elongated Cylinder Cooled by Li-Pb

A. *Structural Material (HT-9) Thickness: 3 mm*

| NODE | TEMP | NODE | TEMP | NODE | TEMP | NODE | TEMP | NODE | TEMP | NODE | TEMP | NODE | TEMP | NODE | TEMP | NODE | TEMP | NODE | TEMP |
|---|---|---|---|---|---|---|---|---|---|---|---|---|---|---|---|---|---|---|---|
| 1 | 304.7 | 2 | 309.0 | 3 | 314.5 | 4 | 321.1 | 5 | 328.1 | 6 | 335.1 | 7 | 341.6 | 8 | 347.2 | 9 | 351.4 | 10 | 354.2 |
| 11 | 303.7 | 12 | 307.9 | 13 | 313.5 | 14 | 320.0 | 15 | 327.1 | 16 | 334.1 | 17 | 340.6 | 18 | 346.2 | 19 | 350.4 | 20 | 353.2 |
| 21 | 301.4 | 22 | 305.7 | 23 | 311.2 | 24 | 317.8 | 25 | 324.8 | 26 | 331.8 | 27 | 333.3 | 28 | 343.9 | 29 | 348.2 | 30 | 350.9 |
| 31 | 309.6 | 32 | 321.3 | 33 | 333.4 | 34 | 344.6 | 35 | 354.1 | 36 | 361.1 | 37 | 365.2 | 38 | 366.0 | 39 | 363.7 | 40 | 359.1 |
| 41 | 315.1 | 42 | 332.0 | 43 | 348.7 | 44 | 363.3 | 45 | 374.6 | 46 | 381.6 | 47 | 383.8 | 48 | 381.3 | 49 | 374.4 | 50 | 364.4 |
| 51 | 320.0 | 52 | 342.2 | 53 | 363.5 | 54 | 381.4 | 55 | 394.4 | 56 | 401.3 | 57 | 401.8 | 58 | 395.9 | 59 | 384.5 | 60 | 369.3 |
| 61 | 335.3 | 62 | 375.5 | 63 | 412.7 | 64 | 442.2 | 65 | 461.2 | 66 | 468.1 | 67 | 462.5 | 68 | 445.1 | 69 | 417.7 | 70 | 384.4 |
| 71 | 336.7 | 72 | 379.1 | 73 | 418.1 | 74 | 443.9 | 75 | 468.6 | 76 | 475.6 | 77 | 469.3 | 78 | 450.5 | 79 | 421.3 | 80 | 385.9 |

B. Structural Material (HT-9) Thickness: 4.5 mm

| NODE | TEMP | NODE | TEMP | NODE | TEMP | NODE | TEMP | NODE | TEMP | NODE | TEMP | NODE | TEMP | NODE | TEMP | NODE | TEMP | NODE | TEMP |
|---|---|---|---|---|---|---|---|---|---|---|---|---|---|---|---|---|---|---|---|
| 1 | 304.8 | 2 | 309.3 | 3 | 315.1 | 4 | 321.9 | 5 | 329.1 | 6 | 336.4 | 7 | 343.2 | 8 | 349.0 | 9 | 353.4 | 10 | 356.4 |
| 11 | 303.8 | 12 | 308.3 | 13 | 314.1 | 14 | 320.8 | 15 | 328.1 | 16 | 335.4 | 17 | 342.1 | 18 | 347.9 | 19 | 352.4 | 20 | 355.4 |
| 21 | 301.5 | 22 | 306.0 | 23 | 311.8 | 24 | 318.6 | 25 | 325.8 | 26 | 333.1 | 27 | 339.9 | 28 | 345.7 | 29 | 350.2 | 30 | 353.1 |
| 31 | 312.6 | 32 | 325.8 | 33 | 339.3 | 34 | 351.7 | 35 | 361.9 | 36 | 369.1 | 37 | 372.9 | 38 | 373.1 | 39 | 369.8 | 40 | 364.1 |
| 41 | 321.5 | 42 | 342.6 | 43 | 363.1 | 44 | 380.5 | 45 | 393.3 | 46 | 400.5 | 47 | 401.7 | 48 | 396.8 | 49 | 386.5 | 50 | 372.9 |
| 51 | 329.3 | 52 | 353.2 | 53 | 383.6 | 54 | 403.0 | 55 | 423.4 | 56 | 430.6 | 57 | 429.0 | 58 | 419.1 | 59 | 402.0 | 60 | 380.6 |
| 61 | 345.8 | 62 | 393.9 | 63 | 433.3 | 64 | 473.0 | 65 | 494.9 | 66 | 502.0 | 67 | 494.0 | 68 | 471.8 | 69 | 437.7 | 70 | 396.9 |
| 71 | 347.3 | 72 | 397.5 | 73 | 443.7 | 74 | 479.7 | 75 | 502.3 | 76 | 509.5 | 77 | 500.8 | 78 | 477.2 | 79 | 441.2 | 80 | 398.4 |

C. Structural Material (HT-9) Thickness: 6 mm

| NODE | TEMP | NODE | TEMP | NODE | TEMP | NODE | TEMP | NODE | TEMP | NODE | TEMP | NODE | TEMP | NODE | TEMP | NODE | TEMP | NODE | TEMP |
|---|---|---|---|---|---|---|---|---|---|---|---|---|---|---|---|---|---|---|---|
| 1 | 305.1 | 2 | 310.1 | 3 | 316.5 | 4 | 323.8 | 5 | 331.6 | 6 | 339.5 | 7 | 346.8 | 8 | 353.1 | 9 | 358.1 | 10 | 361.7 |
| 11 | 304.1 | 12 | 309.1 | 13 | 315.4 | 14 | 322.3 | 15 | 330.6 | 16 | 338.4 | 17 | 345.7 | 18 | 352.1 | 19 | 357.1 | 20 | 360.6 |
| 21 | 301.8 | 22 | 306.8 | 23 | 313.2 | 24 | 320.5 | 25 | 328.3 | 26 | 336.2 | 27 | 343.5 | 28 | 349.8 | 29 | 354.9 | 30 | 358.4 |
| 31 | 318.2 | 32 | 333.2 | 33 | 348.6 | 34 | 362.4 | 35 | 373.6 | 36 | 381.4 | 37 | 385.3 | 38 | 385.1 | 39 | 381.1 | 40 | 374.6 |
| 41 | 332.7 | 42 | 358.2 | 43 | 382.8 | 44 | 403.4 | 45 | 413.1 | 46 | 425.9 | 47 | 426.2 | 48 | 419.2 | 49 | 405.9 | 50 | 388.9 |
| 51 | 344.5 | 52 | 380.2 | 53 | 414.0 | 54 | 441.1 | 55 | 459.3 | 56 | 467.0 | 57 | 463.8 | 58 | 450.2 | 59 | 427.8 | 60 | 400.5 |
| 61 | 362.2 | 62 | 418.3 | 63 | 470.1 | 64 | 510.4 | 65 | 535.5 | 66 | 543.2 | 67 | 533.0 | 68 | 506.3 | 69 | 465.8 | 70 | 418.0 |
| 71 | 363.6 | 72 | 421.9 | 73 | 475.5 | 74 | 517.2 | 75 | 542.9 | 76 | 550.6 | 77 | 539.8 | 78 | 511.7 | 79 | 469.3 | 80 | 419.4 |

The surface heat flux on the first wall is assumed to have a cos $\phi$ distribution ($\phi$ = angle away from the midpoint of each semi-cylinder. Assuming uniform flux distribution in the lengthwise direction of the blanket modules, the thermal analysis was carried out based on two-dimensional heat conduction. The module was divided into ten regions in the circumferential direction, with two layers in the beryllium coating, three in the structural material, one in the coolant, and two in the baffle plate. The baffle plate between the first wall and the blanket region is assumed to be perforated to prevent stagnant thermal regions behind the baffle.

RESULTS OF THERMAL/HYDRAULIC ANALYSIS

The steady-state temperature distribution for three thicknesses of HT-9 structure are given in Table I. Typical temperature plots for a selected set of nodes from the 80-node geometrical model for the 3-mm thickness reference case are shown in Figs. 3 and 4. The results show that ~33% of the total temperature rise of the coolant (20% due to surface heat flux and 13% due to bulk heating) occurs across the first wall. The maximum surface temperature of the structural material (HT-9) reaches ~415°C (obtained by extrapolation from nodes 47 and 57). The maximum surface temperature of the beryllium coating approaches 485°C. The maximum temperature of the structural material at the liquid metal interface occurs at the coolant exit where it approaches the coolant temperature.

The gravity load on a particular first wall/blanket module will depend on its location in the poloidal plane. Hence, the required material thickness will depend to some extent on the location of the modules. A set of calculations was carried out by varying the thickness of the first wall to estimate how the material thickness affects the temperature distribution. When this thickness is increased from 3 to 4.5 mm, and then to 6 mm, the maximum structural material temperature is increased by 33°C and 75°C, respectively. An examination of the circumferential temperature distribution shown in Fig. 4

TABLE I

Steady-State Temperature Distribution in Elongated Cylinder Cooled by Li-Pb

A. Structural Material (HT-9) Thickness: 3 mm

| NODE | TEMP | NODE | TEMP | NODE | TEMP | NODE | TEMP | NODE | TEMP | NODE | TEMP | NODE | TEMP | NODE | TEMP | NODE | TEMP | NODE | TEMP |
|---|---|---|---|---|---|---|---|---|---|---|---|---|---|---|---|---|---|---|---|
| 1 | 304.7 | 2 | 309.0 | 3 | 314.5 | 4 | 321.1 | 5 | 328.1 | 6 | 335.1 | 7 | 341.6 | 8 | 347.2 | 9 | 351.4 | 10 | 354.2 |
| 11 | 303.7 | 12 | 307.9 | 13 | 313.5 | 14 | 320.0 | 15 | 327.1 | 16 | 334.1 | 17 | 340.6 | 18 | 346.2 | 19 | 350.4 | 20 | 353.2 |
| 21 | 301.4 | 22 | 305.7 | 23 | 311.2 | 24 | 317.8 | 25 | 324.8 | 26 | 331.8 | 27 | 338.3 | 28 | 343.9 | 29 | 348.2 | 30 | 350.9 |
| 31 | 309.6 | 32 | 321.3 | 33 | 333.4 | 34 | 344.6 | 35 | 354.1 | 36 | 361.1 | 37 | 365.2 | 38 | 366.0 | 39 | 363.7 | 40 | 359.1 |
| 41 | 315.1 | 42 | 332.0 | 43 | 348.7 | 44 | 363.3 | 45 | 374.6 | 46 | 381.6 | 47 | 383.8 | 48 | 381.3 | 49 | 374.4 | 50 | 364.4 |
| 51 | 320.0 | 52 | 342.2 | 53 | 363.5 | 54 | 381.4 | 55 | 394.4 | 56 | 401.3 | 57 | 401.8 | 58 | 395.9 | 59 | 384.5 | 60 | 369.3 |
| 61 | 335.3 | 62 | 375.5 | 63 | 412.7 | 64 | 442.2 | 65 | 461.2 | 66 | 468.1 | 67 | 462.5 | 68 | 445.1 | 69 | 417.7 | 70 | 384.4 |
| 71 | 336.7 | 72 | 379.1 | 73 | 418.1 | 74 | 448.9 | 75 | 468.6 | 76 | 475.6 | 77 | 469.3 | 78 | 450.5 | 79 | 421.3 | 80 | 383.9 |

B. Structural Material (HT-9) Thickness: 4.5 mm

| NODE | TEMP | NODE | TEMP | NODE | TEMP | NODE | TEMP | NODE | TEMP | NODE | TEMP | NODE | TEMP | NODE | TEMP | NODE | TEMP | NODE | TEMP |
|---|---|---|---|---|---|---|---|---|---|---|---|---|---|---|---|---|---|---|---|
| 1 | 304.8 | 2 | 309.3 | 3 | 315.1 | 4 | 321.9 | 5 | 329.1 | 6 | 336.4 | 7 | 343.2 | 8 | 349.0 | 9 | 353.4 | 10 | 356.4 |
| 11 | 303.8 | 12 | 308.3 | 13 | 314.1 | 14 | 320.8 | 15 | 328.1 | 16 | 335.4 | 17 | 342.1 | 18 | 347.9 | 19 | 352.4 | 20 | 355.4 |
| 21 | 301.5 | 22 | 306.0 | 23 | 311.8 | 24 | 318.6 | 25 | 325.8 | 26 | 333.1 | 27 | 339.9 | 28 | 345.7 | 29 | 350.2 | 30 | 353.1 |
| 31 | 312.6 | 32 | 325.8 | 33 | 339.3 | 34 | 351.7 | 35 | 361.9 | 36 | 369.1 | 37 | 372.9 | 38 | 373.1 | 39 | 369.8 | 40 | 364.1 |
| 41 | 321.5 | 42 | 342.6 | 43 | 363.1 | 44 | 380.5 | 45 | 393.3 | 46 | 400.5 | 47 | 401.7 | 48 | 396.8 | 49 | 386.5 | 50 | 372.9 |
| 51 | 329.3 | 52 | 353.2 | 53 | 385.6 | 54 | 408.0 | 55 | 423.4 | 56 | 433.6 | 57 | 429.0 | 58 | 419.1 | 59 | 402.0 | 60 | 380.6 |
| 61 | 345.8 | 62 | 393.9 | 63 | 433.5 | 64 | 473.0 | 65 | 494.9 | 66 | 502.0 | 67 | 494.0 | 68 | 471.8 | 69 | 437.7 | 70 | 396.9 |
| 71 | 347.3 | 72 | 397.5 | 73 | 443.7 | 74 | 479.7 | 75 | 502.3 | 76 | 509.5 | 77 | 500.8 | 78 | 477.2 | 79 | 441.2 | 80 | 398.4 |

C. Structural Material (HT-9) Thickness: 6 mm

| NODE | TEMP | NODE | TEMP | NODE | TEMP | NODE | TEMP | NODE | TEMP | NODE | TEMP | NODE | TEMP | NODE | TEMP | NODE | TEMP | NODE | TEMP |
|---|---|---|---|---|---|---|---|---|---|---|---|---|---|---|---|---|---|---|---|
| 1 | 305.1 | 2 | 310.1 | 3 | 316.5 | 4 | 323.8 | 5 | 331.6 | 6 | 339.5 | 7 | 346.8 | 8 | 353.1 | 9 | 358.1 | 10 | 361.7 |
| 11 | 304.1 | 12 | 309.1 | 13 | 315.4 | 14 | 322.8 | 15 | 330.6 | 16 | 338.4 | 17 | 345.7 | 18 | 352.1 | 19 | 357.1 | 20 | 360.6 |
| 21 | 301.8 | 22 | 306.8 | 23 | 313.2 | 24 | 320.5 | 25 | 328.3 | 26 | 336.2 | 27 | 343.5 | 28 | 349.8 | 29 | 354.9 | 30 | 358.4 |
| 31 | 318.2 | 32 | 333.2 | 33 | 348.6 | 34 | 362.4 | 35 | 373.6 | 36 | 381.4 | 37 | 385.3 | 38 | 385.1 | 39 | 381.1 | 40 | 374.6 |
| 41 | 332.7 | 42 | 358.2 | 43 | 382.8 | 44 | 403.4 | 45 | 418.1 | 46 | 425.9 | 47 | 426.2 | 48 | 419.2 | 49 | 405.9 | 50 | 388.9 |
| 51 | 344.5 | 52 | 380.2 | 53 | 414.0 | 54 | 441.1 | 55 | 459.3 | 56 | 467.0 | 57 | 463.8 | 58 | 450.2 | 59 | 427.8 | 60 | 400.5 |
| 61 | 352.2 | 62 | 418.3 | 63 | 470.1 | 64 | 510.4 | 65 | 535.5 | 66 | 543.2 | 67 | 533.0 | 68 | 506.3 | 69 | 465.8 | 70 | 418.0 |
| 71 | 363.6 | 72 | 421.9 | 73 | 475.5 | 74 | 517.2 | 75 | 542.9 | 76 | 550.6 | 77 | 539.8 | 78 | 511.7 | 79 | 469.3 | 80 | 419.4 |

distribution was calculated by varying the contact coefficient between 1 and 10 $W/cm^2$-K. The results show that when the contact coefficient is increased by a factor of 10, the coating temperature decreases by ~45°C.

## RESULTS OF STRUCTURAL ANALYSIS

A preliminary elastic stress analysis was performed to determine the structural requirement for a typical double-head module. In terms of determining strucural arrangement and thicknesses, the internal pressure is the most important applied load. Coolant pressure was assumed to be 1.4 MPa, due both to static head from interconnected modules and to pumping head pressure. Temperature distributions from the thermal hydraulic analysis described above were used to determine thermal streses. Both HT-9 and V-alloy were examined as structural materials. Allowable sresses were based on methods developed from Sec. III of the ASME Code, except that as a simplification thermal stresses and primary stresses were each limited to 1.5 $S_m$.

The selected structural configuration is shown in Fig. 1. The internal pressure acts on the side walls which beam this load to the internal frames. For modules with differences in side wall loads due to internal static head difference and breeder gravity loads, the frames react these loads in shear to the back wall. Even though the side walls are cylindrical in the first wall section, the principal load path in the skin for internal pressure is still in the toroidal direction, since the skin beams the pressure to the tension webs.

Thermal stresses calculated for the temperature conditions in Fig. 5 consisted of two parts: (2) local thermal stress $(\sigma_{tl})$ due to ΔT through the wall thickness; and (2) overall thermal stress $(\sigma_{to})$ due to ΔT on the blanket cross section (stress in toroidal direction). Temperature variation through the thickness is nearly linear, and a simple plate relationship was used. The baseline configuration analyzed has a through-thickness ΔT of 63°C, resulting in a local thermal sress for HT-9 of 94.6 MPa or about one-third of the assumed allowable secondary stress (1.5 $S_m$). Overall thermal stresses were elastically calculated for the blanket module cross section, assuming the blanket module is unconstrained either in axial extension or in bending. The maximum overall thermal stress (151 MPa) occurs in the cusp area on the inboard wall, and represents about two-thirds of the assumed allowable secondary stress (1.5 $S_m$).

| ELE. | TEMP. (°C) | THERMAL STRESS |
|---|---|---|
| 1 | 300 | 151 MPa |
| 2 | 315 | 107 |
| 3 | 332 | 60 |
| 4 | 349 | 15 |
| 5 | 363 | −23 |
| 6 | 374 | −52 |
| 7 | 381 | −67 |
| 8 | 384 | −68 |
| 9 | 381 | −56 |
| 10 | 374 | −33 |
| 11 | 364 | − 1 |
| 12 | 370 | − 1 |
| 13 | 378 | − 1 |
| 14 | 385 | − 1 |
| 15 | 392 | − 1 |
| 16 | 399 | − 1 |
| 17 | 406 | − 1 |
| 18 | 414 | − 1 |
| 19 | 421 | − 1 |
| 20 | 428 | − 2 |
| 21 | 435 | − 2 |
| 22 | 444 | − 2 |
| 23 | 450 | − 4 |
| 24 | 450 | − 4 |
| 25 | 450 | − 4 |
| 26 | 450 | − 4 |
| 27 | 450 | − 4 |

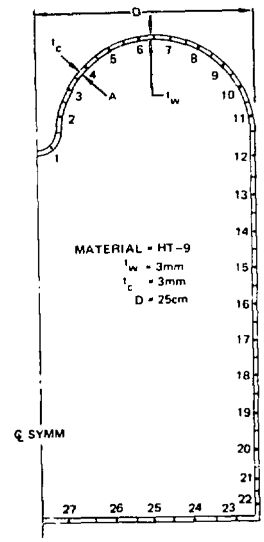


Fig. 5. Blanket module overall thermal stresses.

Sensitivity studies performed for both candidate structural materials showed that, in order to maximize the allowable coolant temperature rise, it is desirable to minimize the side-wall thickness and first-wall half cylinder diameter, and also to minimize the first-wall coolant channel width. The V-alloy can be used at higher temperatures than HT-9 because it has a higher allowable stress and lower thermal stress. Thus, the vanadium alloy can be used with a significantly higher coolant temperature rise (and thus a higher energy conversion efficiency) for a given side wall thickness.

## SUMMARY AND CONCLUSIONS

A series of comparative thermal hydraulic calculations for the self-cooled Li-Pb breeding blanket was carried out for HT-9 and vanadium alloy as the structural materials. The parametric studies considered variations in thickness of the structural material, coolant channel thickness, diameter of the cylindrical blanket modules, interfacial contact resistance between the coating and the structural material, and the temperature rise for the coolant. Because of the modest heat flux for the DEMO first wall/blanket modules, there appear to be no structural problems from the standpoint of temperature limits even for the lower limit of interfacial contact coefficient. For most of the cases included in this analysis the coolant outlet temperature appears to set the structural maximum temperature. By using wider coolant channels, which reduces the required coolant velocities, the MHD pressure losses can be minimized. If 450°C is assumed to be the upper temperature limit for HT-9, then the coolant temperature rise would be limited to 150°C. For the V-alloy the coolant temperature rise may be as high as 250°C. The 3-mm thickness of the beryllium coating resulted in a maximum temperature of 485°C for the reference case. Thicker coatings can be used if necessary for longer surface erosion lifetimes.

From the results of the thermal-hydraulic and stress analyses it can be concluded that the elongated cylindrical blanket modules made from HT-9 or V-alloy appear to offer a viable design concept. Analysis of the intermediate heat exchangers, fluid transport and power conversion systems, and tritium containment and extraction systems are necessary to complete the evaluation.

## ACKNOWLEDGMENT

This work was supported by the U. S. Department of Energy.

## REFERENCES

1. B. BADGER, et al., "UWMAK-III, A Non-Circular Power Reactor Design," UWFDM-150, University of Wisconsin (1976).
2. C. C. BAKER, et al., "STARFIRE - A Commercial Tokamak Fusion Power Plant Study," ANL/FPP-80-1 (1980).
3. W. M. STACEY, JR., et al., "U.S.-INTOR Contribution to the International Tokamak Reactor Phase I Conceptual Design," US-INTOR-81-1 (1981).
4. M. A. ABDOU, et al., "A Demonstration Tokamak Power Plant Study (DEMO)," ANL/FPP-82-1, Argonne National Laboratory (1982).
5. D. L. SMITH, et al., "Fusion Reactor Blanket/Shield Design Study," ANL/FPP-79-1, Argonne National Laboratory (1979).